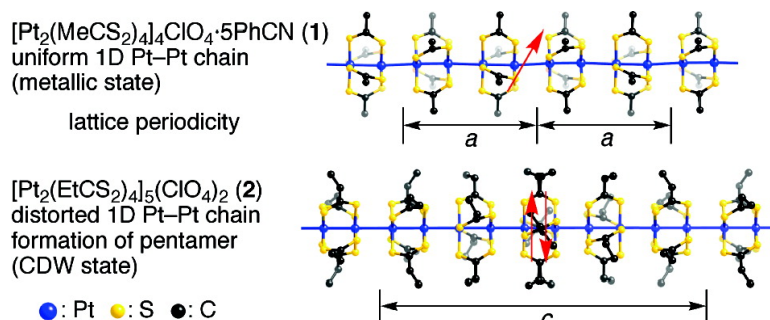


Constructing Highly Conducting Metal#Metal Bonded Solids by Electrocrystallization of [Pt(RCS)] (RCS = Dithiocarboxylato, R = Methyl or Ethyl)

Minoru Mitsumi, Hidekazu Ueda, Kazumi Furukawa,
 Yoshiki Ozawa, Koshiro Toriumi, and Mohamedally Kurmoo

J. Am. Chem. Soc., **2008**, 130 (43), 14102-14104 • DOI: 10.1021/ja805794a • Publication Date (Web): 04 October 2008

Downloaded from <http://pubs.acs.org> on February 8, 2009



More About This Article

Additional resources and features associated with this article are available within the HTML version:

- Supporting Information
- Access to high resolution figures
- Links to articles and content related to this article
- Copyright permission to reproduce figures and/or text from this article

[View the Full Text HTML](#)

Constructing Highly Conducting Metal–Metal Bonded Solids by Electrocrystallization of $[\text{Pt}^{\text{II}}_2(\text{RCS}_2)_4]$ ($\text{RCS}_2^- = \text{Dithiocarboxylato}$, $\text{R} = \text{Methyl}$ or Ethyl)

Minoru Mitsumi,^{*,†} Hidekazu Ueda,[†] Kazumi Furukawa,[†] Yoshiki Ozawa,[†] Koshiro Toriumi,^{*,†} and Mohamedally Kurmoo[‡]

Department of Material Science, Graduate School of Material Science, University of Hyogo, 3-2-1 Kouto, Kamigori-cho, Ako-gun, Hyogo 678-1297, Japan, and Laboratoire de Chimie de Coordination Organique, CNRS-UMR 7140, Université Louis Pasteur, 4 rue Blaise Pascal, F-67000 Strasbourg, France

Received July 24, 2008; E-mail: mitsumi@sci.u-hyogo.ac.jp

Mixed valency (MV) is at the heart of many interesting properties, electrical, magnetic, and optical or combination thereof, and is in many cases the source of a wide range of instabilities. While the properties have been of interest in making devices for particular applications, the instabilities have remained of academic interest. The presence of MV has been the driving force in the development of highly conducting and superconducting materials, molecular magnetism, and also of highly colored complexes.¹ MV was first realized in inorganic compounds and, in particular, one-dimensional (1D) chain compounds of platinum. Most 1D mixed-valent metal complexes are semiconducting except for $\text{K}_2[\text{Pt}(\text{CN})_4]\text{Br}_{0.3} \cdot 3\text{H}_2\text{O}$ (KCP(Br)) and $\text{K}_{1.62}[\text{Pt}(\text{C}_2\text{O}_4)_2] \cdot 2\text{H}_2\text{O}$ (α -K-OP) which shows metallic conduction in a limited range of temperature.^{2,3} On the other hand, MV is also encountered in organics and it has been well-developed in the chemistry of TTF, tetrathiafulvalene, and its derivatives.⁴ The TTF family of materials is more stable through the range of oxidation states and higher dimensionality which are brought about principally by the different modes of stacking of the planar molecules with intermolecular interactions through the chalcogenides. Combining the two systems, that is establishing a Pt spine with planar arrangement of chalcogenides around it, is expected to prevent certain instabilities thus promoting higher conductivity and stability to lower temperatures. Our approach to construct highly conducting metal–metal bonded solids is, therefore, to start with a platinum dimer having sulfur ligands, such as $[\text{Pt}^{\text{II}}_2(\text{RCS}_2)_4]$ ($\text{RCS}_2^- = \text{a dithiocarboxylato}$), and to partially oxidize it in the absence of halide ions. The presence of halide favors the 1D halogen-bridged mixed-valent MM–X compounds, which also suffer from the Peierls instability due to the half-filled band formation.⁵ Here, we used ClO_4^- as a counterion in the electrocrystallization and organic solvents. In choosing the divalent Pt–Pt dimer, we expect a decrease in the Coulomb repulsion U by sharing an unpaired electron through a Pt–Pt bond and the presence of the delocalized sulfur orbitals should favor an increase of the charge-transfer energy t .

Following the above strategy, we have succeeded in obtaining high-quality crystals of the partially oxidized 1D Pt–Pt chain compounds, $[\text{Pt}_2(\text{MeCS}_2)_4]\text{ClO}_4 \cdot 5\text{PhCN}$ (**1**) and $[\text{Pt}_2(\text{EtCS}_2)_4]_5(\text{ClO}_4)_2$ (**2**) from the corresponding dimers. Herein, we report their syntheses, crystal structures, and solid-state properties. Although the structures are closely related, the number of ClO_4^- per dimer and their positions are different. Consequently, the valence state of the platinum atoms and the periodicity of the 1D chain are different and result in metallic behavior for **1** and semiconducting

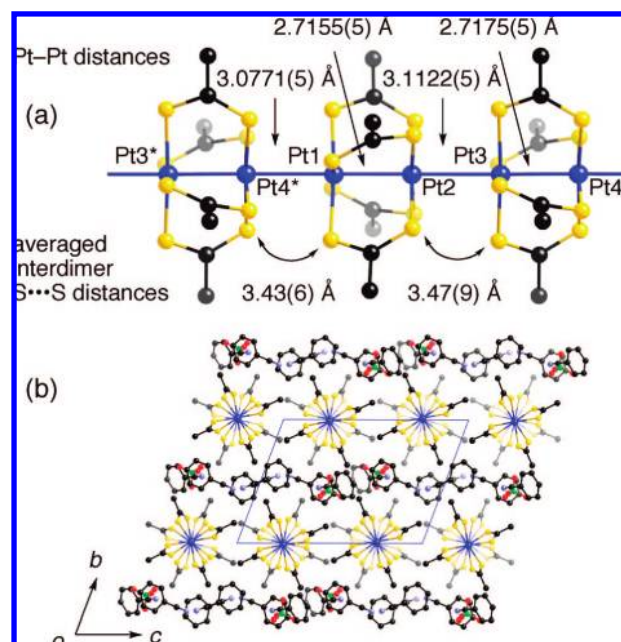


Figure 1. (a) A repeat unit of the 1D chain $\{[\text{Pt}_2(\text{MeCS}_2)_4]_n\}^{n+}$ in **1** at 204 K and (b) view of the unit cell along the chain axis (a axis).

behavior for **2**. **1** sustains metallic conduction to a lower temperature than KCP(Br) and is, to our knowledge, the most stable ambient pressure metallic 1D mixed-valent metal complex known.

Long dark green plate crystals of **1** were obtained by electrochemical oxidation of $[\text{Pt}_2(\text{MeCS}_2)_4]$ ⁶ in benzonitrile with $n\text{-Bu}_4\text{NClO}_4$ as electrolyte. Black prismatic crystals of **2** were likewise obtained from $[\text{Pt}_2(\text{EtCS}_2)_4]$ ^{5c} in chlorobenzene.

The Pt $4f_{7/2}$ and $4f_{5/2}$ bands in the X-ray photoelectron spectra (XPS) of **1** and **2** are slightly broader than those of the diplatinum (II) complex $[\text{Pt}_2(\text{EtCS}_2)_4]$ (Figure S1, Table S2). These bands for **1** and **2** can be well resolved into $\text{Pt}^{2+} 4f_{7/2,5/2}$ and $\text{Pt}^{3+} 4f_{7/2,5/2}$ doublets, confirming that **1** and **2** exist in the mixed-valence state on a rapid time scale (ca. 10^{-17} s).

Crystal structures were determined from data collected on single crystals of **1** and **2** using synchrotron radiation of the BL02B1 beamline at SPring-8. The structure of **1** (triclinic, $P\bar{1}$) consists of alternating cationic and solvated anionic layers; the former is built of stacks of Pt–Pt dimers forming chains adjacent to one another while the latter contains ClO_4^- solvated by benzonitrile molecules (Figure 1). One period of the linear chain has two diplatinum units with two independent Pt–Pt distances, Pt1–Pt2 2.7155(5) Å and Pt3–Pt4 2.7175(5) Å. It is known that the intradimer Pt–Pt distance

[†] University of Hyogo.

[‡] Université Louis Pasteur.

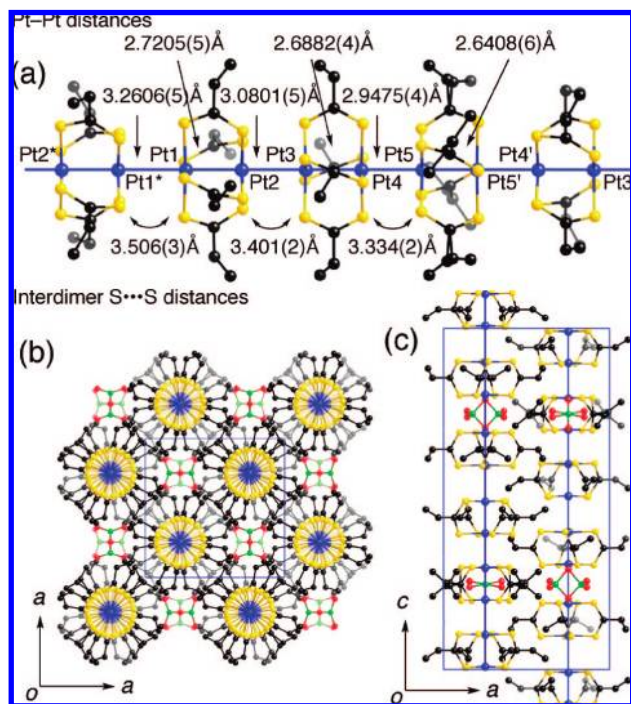


Figure 2. (a) A repeat unit of the 1D chain $\{[\text{Pt}_2(\text{EtCS}_2)_4]_5\}_n^{2n+}$ in **2** at 298 K and a view of the packing projected down the (b) *c* and (c) *a* axes.

depends on the valence state of a diplatinum unit, e.g., 2.767(1) Å for $[\text{Pt}_2^{\text{II,III}}(\text{MeCS}_2)_4]$ and 2.677(2) Å for $[\text{Pt}_2^{\text{II,III}}(\text{MeCS}_2)_4]_\infty$.^{5a,6} The intradimer Pt–Pt distances of **1** are intermediate between those of Pt^{2+} – Pt^{2+} and Pt^{2+} – Pt^{3+} while the interdimer Pt–Pt distances are longer, Pt1–Pt4* 3.0771(5) Å and Pt2–Pt3 3.1122(5) Å. The Pt–Pt dimers are almost equidistant from one another forming the spine with notably short interdimer S···S distances. Adjacent dimers are twisted by 44° with respect to MeCS_2^- to avoid the steric hindrance between sulfur atoms. The effect of the charged ClO_4^- being insulated by the benzonitrile molecules could be the reason why the Pt–Pt chains are almost regular. The molar ratio of the $\text{Pt}_2(\text{MeCS}_2)_4$ cation to ClO_4^- is 4:1, in agreement with elemental analyses. Therefore, the average formal oxidation state of the platinum atom of **1** is +2.125.

The structure of **2** (tetragonal, $P4/mnc$) is shown in Figure 2, consisting of 1D Pt–Pt chains segregated by ClO_4^- . The diplatinum units are stacked with a twist of the EtCS_2^- ligands forming the Pt–Pt chain with helical arrangement of the ligands. In the Pt–Pt chain, five diplatinum units form a pentamer, and both the intra- and interdimer Pt–Pt distances are shorter at the center of the pentamer (a midpoint of Pt5–Pt5' bond). Intradimer Pt–Pt distances are Pt1–Pt2 = 2.7205(5), Pt3–Pt4 = 2.6882(4), and Pt5–Pt5' = 2.6408(6) Å, respectively, while interdimer Pt–Pt distances are Pt1–Pt1* = 3.2606(5), Pt2–Pt3 = 3.0801(5), and Pt4–Pt5 = 2.9475(4) Å. The Pt–Pt distances of $[\text{Pt}_2^{\text{II,III}}(\text{EtCS}_2)_4]$, $[\text{Pt}_2^{\text{II,III}}(\text{EtCS}_2)_4]_\infty$, and $[\text{Pt}_2^{\text{III,III}}(\text{EtCS}_2)_4\text{I}_2]$ are 2.764(1), 2.684(1), and 2.582(1) Å, respectively.^{5e,7} By comparing the intradimer Pt–Pt distances of **2**, it is apparent that the Pt1–Pt2 distance is intermediate between those of Pt^{2+} – Pt^{2+} and Pt^{2+} – Pt^{3+} , the Pt3–Pt4 distance is close to that of Pt^{2+} – Pt^{3+} , and the Pt5–Pt5' distance is intermediate between those of Pt^{2+} – Pt^{3+} and Pt^{3+} – Pt^{3+} . Furthermore, there are short interdimer S···S contacts in the 1D chain. When **2** takes a similar stacking pattern as that for **1**, the spaces surrounded by 1D chains will increase due to the elongation of the alkyl moiety. Therefore, **2** appears to adopt the

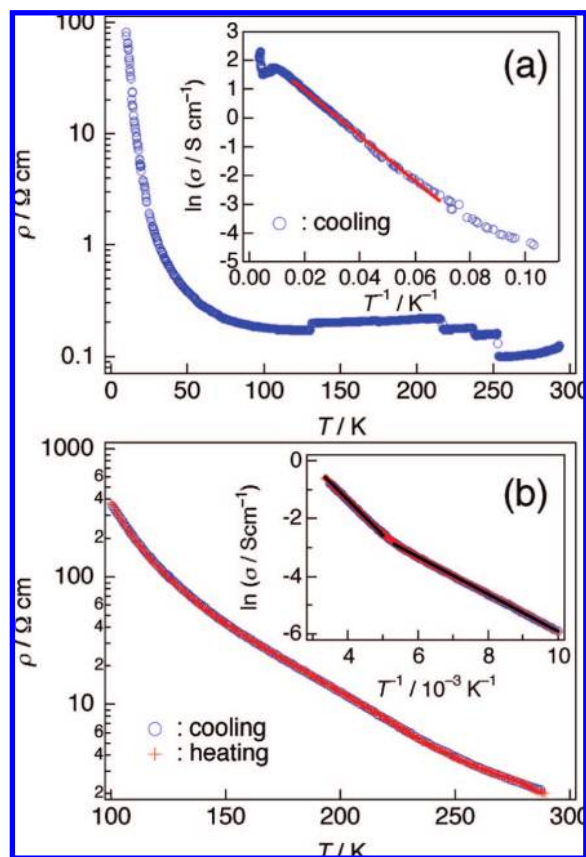


Figure 3. Temperature dependence of electrical resistivity ρ and electrical conductivity σ along 1D chain direction of (a) **1** and (b) **2**.⁸

helical arrangement of EtCS_2^- for efficient packing, and the ClO_4^- ions are incorporated simultaneously into the spaces formed partially by four 1D chains (Figure S2). Consequently, the interdimer Pt···Pt distance adjacent to ClO_4^- is lengthened by the steric hindrance. Therefore, it is considered that the periodicity of the helical arrangement of the ligands is strongly correlated with the number of ClO_4^- ions. Since the molar ratio of $\text{Pt}_2(\text{EtCS}_2)_4$ to ClO_4^- has been confirmed to be 5:2 by elemental analyses, the average oxidation number of the platinum atoms of **2** is +2.2.

Solid-state vis–NIR–IR spectra of **1** and **2** exhibit relatively strong broad absorption bands centered at ca. 3400 and 4100 cm^{-1} , respectively, which are not observed in the Pt(II) dimers $[\text{Pt}_2(\text{MeCS}_2)_4]$ and $[\text{Pt}_2(\text{EtCS}_2)_4]$ (Figure S3). These bands are attributed to the interdimer charge-transfer absorption, $d\sigma^{*1}d\sigma^{*2} \leftarrow d\sigma^{*2}d\sigma^{*1}$. These bands extend to the mid-infrared region and thus the low activation energies.

As we anticipated, **1** exhibits high electrical conductivity (4.2–8.0 S cm^{-1}) at room temperature along the 1D chain and metallic behavior surviving down to 125 K (Figure 3) in contrast to 250 K for KCP(Br).^{2a} The resistivity jump observed upon cooling is attributable to the formation of microcracks within the crystal due to the tendency to lose benzonitrile molecules from the crystal surface.⁸ The activation energy E_a in the semiconducting regime ($T = 62.5$ – 14.5 K) is very small, 6.75 meV. The electrical conductivity of **2** is 0.33–1.2 S cm^{-1} at room temperature and shows typical semiconducting behavior (Figure 3). The activation energies are 103 meV ($T = 300$ – 200 K) and 56 meV ($T = 188$ – 100 K). The observed semiconducting behavior of **2** can be ascribed to the electronic localization due to formation of pentamers within the chains.

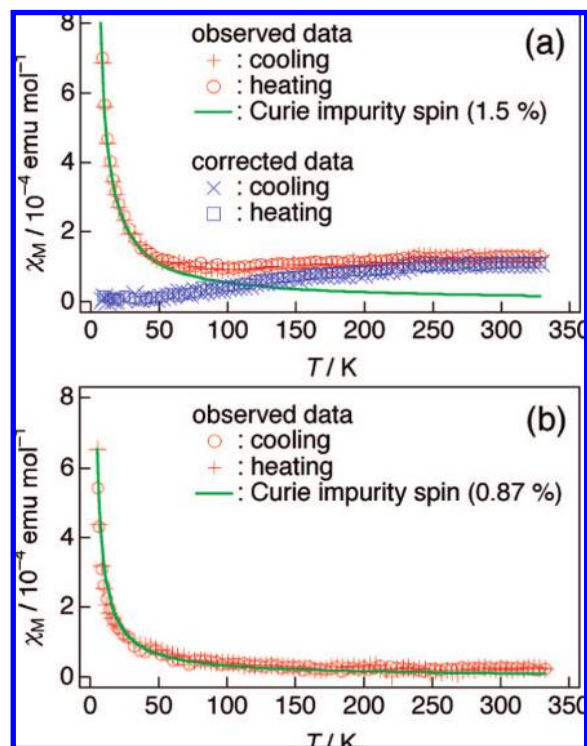


Figure 4. (a) Temperature dependence of magnetic susceptibility χ_M for **1** (red markers), after correction for the Curie impurity contribution (blue markers). (b) Temperature dependence of χ_M for **2**.

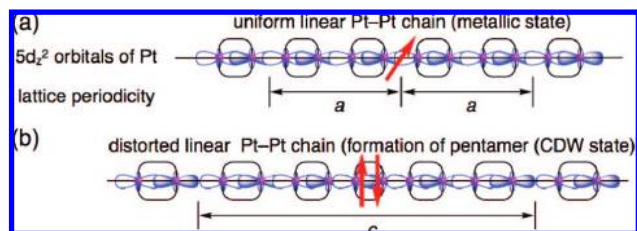


Figure 5. Schematic representation of the spin states and lattice periodicities of the linear Pt–Pt chains for (a) **1** and (b) **2**.

The magnetic susceptibility χ_M of **1** is Pauli-like except for the tail below 30 K, which can account for paramagnetic impurities and/or lattice and end-of-chains defects (Figure 4) and is estimated to be 1.5% assuming the impurity spin of $S = 1/2$. After correction χ_M is almost temperature independent (ca. 1.1×10^{-4} emu mol $^{-1}$) and gradually decreases with lowering temperature to an almost spin-singlet state. On the other hand, **2** appears to be nonmagnetic except for a very small Curie-like paramagnetic behavior originating from impurities and/or lattice and end-of-chains defects.

The difference in electrical properties of **1** and **2** is a consequence of the structure, whereby electronic delocalization is favored by the equidistant separation between dimers due to the lack of cation–anion interactions, whereas localization sets are due to the strong electrostatic cation–anion interaction resulting in very different interdimer separations. From electronic considerations as shown in Figure 5, the one unpaired electron (odd electron) for every four dimers in **1**, i.e. twice the length of the a axis, is unlikely

to pair, and consequently, the charge and spin degrees of freedom survive resulting in metallic conduction. On the other hand, **2** has lost the spin degree of freedom due to the formation of a pentamer with electron pair formation since two unpaired electrons (even electron) are present per unit cell, and the charge density wave (CDW) state has appeared.

We have demonstrated that the presence of a square planar Pt spine with sulfur donor ligands around can stabilize high electrical conductivity and to much lower temperatures. In addition, cation–anion interactions play an important role in electronic localization and, therefore, the control of the charge and spin degrees of freedom.

Acknowledgment. This work was supported by a Grants-in-Aid for Scientific Research from the Hyogo Prefecture and a Research Foundation for Materials Science, SPring-8 (experiments 2003B2888-PU1-np and 2000B0512-ND-np), and CNRS. We are grateful to Dr. H. Akutsu and Profs. J. Yamada, S. Nakatsuji, and M. Kobayashi for the use of their conductivity measurement apparatus.

Supporting Information Available: Crystallographic data, XPS spectra, and vis–NIR–IR spectra of **1** and **2**. This material is available free of charge via the Internet at <http://pubs.acs.org>.

References

- Day, P. *Molecules into Materials: Case Studies in Materials Chemistry—Mixed Valency, Magnetism and Superconductivity*; World Scientific Publishing: Singapore, 2007.
- (a) Zeller, H. R.; Beck, A. *J. Phys. Chem. Solids* **1974**, *35*, 77–80. (b) Kobayashi, A.; Sasaki, Y.; Shirotani, I.; Kobayashi, H. *Solid State Commun.* **1978**, *26*, 653–656.
- For 1D mixed-valent metal complexes, see: (a) Bera, J. K.; Dunbar, K. R. *Angew. Chem., Int. Ed.* **2002**, *41*, 4453–4457. (b) Prater, M. E.; Pence, L. E.; Clérac, R.; Finnis, G. M.; Campana, C.; Auban-Senzier, P.; Jérôme, D.; Canadell, E.; Dunbar, K. R. *J. Am. Chem. Soc.* **1999**, *121*, 8005–8016. (c) Sakai, K.; Ishigami, E.; Konno, Y.; Kajiwara, T.; Ito, T. *J. Am. Chem. Soc.* **2002**, *124*, 12088–12089. (d) Mitsumi, M.; Goto, H.; Umebayashi, S.; Ozawa, Y.; Kobayashi, M.; Yokoyama, T.; Tanaka, H.; Kuroda, S.; Toriumi, K. *Angew. Chem., Int. Ed.* **2005**, *44*, 4164–4168. (e) Uemura, K.; Fukui, K.; Nishikawa, H.; Arai, S.; Matsumoto, K.; Oshio, H. *Angew. Chem., Int. Ed.* **2005**, *44*, 5459–5464.
- Ishiguro, T.; Yamaji, K.; Saito, G. *Organic Superconductors*, 2nd ed; Springer Series in Solid State Sciences 88; Springer: Heidelberg, 1998.
- For 1D halogen-bridged mixed-valent MM-X type complexes, see: (a) Bellitto, C.; Flamini, A.; Gastaldi, L.; Scaramuzza, L. *Inorg. Chem.* **1983**, *22*, 444–449. (b) Kurmoo, M.; Clark, R. J. H. *Inorg. Chem.* **1985**, *24*, 4420–4425. (c) Butler, L. G.; Zietlow, M. H.; Che, C.-M.; Schaefer, W. P.; Sridhar, S.; Grunthaner, P. J.; Swanson, B. I.; Clark, R. J. H.; Gray, H. B. *J. Am. Chem. Soc.* **1988**, *110*, 1155–1162. (d) Kitagawa, H.; Onodera, N.; Sonoyama, T.; Yamamoto, M.; Fukawa, T.; Mitani, T.; Seto, M.; Maeda, Y. *J. Am. Chem. Soc.* **1999**, *121*, 10068–10080. (e) Mitsumi, M.; Murase, T.; Kishida, H.; Yoshinari, T.; Ozawa, Y.; Toriumi, K.; Sonoyama, T.; Kitagawa, H.; Mitani, T. *J. Am. Chem. Soc.* **2001**, *123*, 11179–11192. (f) Mitsumi, M.; Kitamura, K.; Morinaga, A.; Ozawa, Y.; Kobayashi, M.; Toriumi, K.; Iso, Y.; Kitagawa, H.; Mitani, T. *Angew. Chem., Int. Ed.* **2002**, *41*, 2767–2771. (g) Otsubo, K.; Kobayashi, A.; Kitagawa, H.; Hedo, M.; Uwatoko, Y.; Sagayama, H.; Wakabayashi, Y.; Sawa, H. *J. Am. Chem. Soc.* **2006**, *128*, 8140–8141. (h) Yamashita, M.; Takaishi, S.; Kobayashi, A.; Kitagawa, H.; Matsuzaki, H.; Okamoto, H. *Coord. Chem. Rev.* **2006**, *250*, 2335–2346.
- Bellitto, C.; Flamini, A.; Piovesana, O.; Zanazzi, P. F. *Inorg. Chem.* **1980**, *19*, 3632–3636.
- Mitsumi, M.; Yoshinari, T.; Ozawa, Y.; Toriumi, K. *Mol. Cryst. Liq. Cryst.* **2000**, *342*, 127–132.
- The single crystal of **1** is relatively unstable due to the tendency to lose benzonitrile molecules from the crystal surface. Therefore, attempts to measure the temperature dependence of the resistivity of **1** without the formation of microcracks were unsuccessful.

JA805794A